Proc. IEEE Vehicular Technology
Conference Fall 2003 (VTC Fall 2003),
Orlando (FL), Oct. 2003, vol.2, pp. 781-785.

Frequency Synchronization for MIMO OFDM Wireless LAN Systems

Tim C.W. Schenk and Allert van Zelst
Eindhoven University of Technology, PO Box 513, 5600 MB Eindhoven, The Netherlands
Agere Systems, PO Box 755, 3430 AT Nieuwegein, The Netherlands, {tschenk, zelst}@agere.com

***Abstract*— This paper proposes an accurate and time-efficient technique for frequency synchronization of multiple-input multiple-output (MIMO) orthogonal frequency division multiplexing (OFDM) systems. The technique uses a preamble and is thus especially suitable for burst mode communication. The preamble consists of training sequences simultaneously transmitted from the various transmit antennas. From analysis, it is shown that the accuracy of frequency synchronization is close to the Cramér-Rao lower bound and increases for increasing rms delay spreads and number of receive antennas. Furthermore, application of the proposed algorithm in MIMO OFDM wireless local-area-network (WLAN) systems leads to a BER that is only slightly higher than that of a perfectly synchronized system, making it highly applicable.**

I. Introduction

The main reasons why orthogonal frequency division multiplexing (OFDM) was adopted in the wireless local-area-network (WLAN) standards IEEE 802.11a [1] and g [2] are its high spectral efficiency and ability to deal with frequency selective fading and narrowband interference. The combination of OFDM with spectral efficient multiple antenna techniques, also know as multiple-input multiple-output (MIMO) [3], opens the door to high data-rate wireless communication [4]. The indoor deployment of WLANs makes MIMO OFDM a strong candidate for high throughput extensions of current WLAN standards, since the throughput enhancement of MIMO is especially high in richly-scattered scenarios of which indoor environments are typical examples.

Similar to a single-input single-output (SISO) OFDM system, a multi-antenna OFDM system is very sensitive to carrier frequency offset (CFO), which introduces inter-carrier-interference (ICI) [5], [6]. Accurate frequency synchronization is thus essential for reliable reception of the transmitted data. Various carrier synchronization schemes have been proposed for SISO OFDM systems. Some schemes rely on pilot or preamble data [6]–[8] and some use the inherent structure of the OFDM symbol in either frequency [9] or time domain [10]. For multiple antenna OFDM data-aided schemes are proposed for receiver diversity and MIMO in [11] and [12], respectively. A blind method for receiver diversity combined with OFDM is proposed in [13].

This paper elaborates on ideas from [11] and [12] resulting in a data-aided frequency synchronization approach for MIMO OFDM systems. In addition to [12], we analytically show the tradeoff between estimation accuracy on the one hand and preamble length and number of antennas on the other hand, which is facilitated by the design of a scalable preamble. Furthermore, we more extensively explore the performance gains in multipath environments by means of simulations.

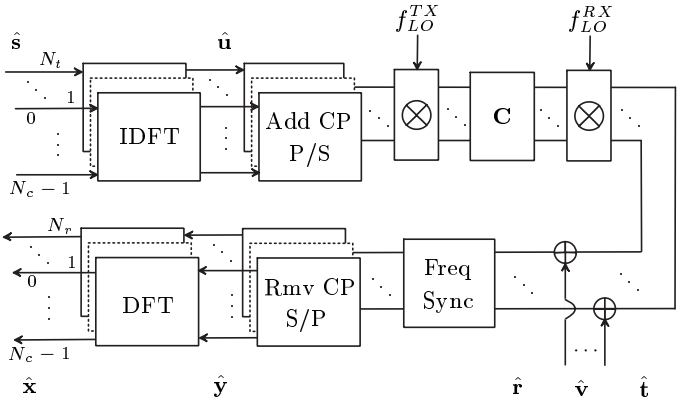

Fig. 1. MIMO OFDM system model with frequency synchronization.

The layout of the paper is as follows. In Section II the MIMO OFDM signal model is defined and the influence of CFO is shown. Section III introduces the preamble and frequency synchronization algorithm. The performance is evaluated analytically and numerically in Section IV and Section V, respectively. Finally, conclusions are drawn in Section VI.

II. MIMO OFDM signal model

Suppose that a communication system consists of N_t transmit (TX) and N_r receive (RX) antennas, denoted as a $N_t \times N_r$ system. Figure 1 depicts such a system. Let us define the a-th MIMO OFDM vector to be transmitted as $\hat{\mathbf{s}}(a) = \text{vec}\left(\mathbf{s}(0,a), \mathbf{s}(1,a), \ldots, \mathbf{s}(N_c-1,a)\right)$, where $\mathbf{s}(n,a)$ denotes the $N_t \times 1$ frequency domain MIMO transmit vector for the n-th subcarrier and N_c represents the number of subcarriers. This vector is transformed to the time domain using the inverse discrete Fourier transform (IDFT)

$$\hat{\mathbf{u}}(a) = \left(\mathbf{F}^{-1} \otimes \mathbf{I}_{N_t}\right) \hat{\mathbf{s}}(a) \ , \tag{1}$$

where $\otimes$ denotes the Kronecker Product, $\mathbf{F}$ is the $N_c \times N_c$ Fourier matrix, of which the (i,k)-th element equals $\exp(-j2\pi\frac{ik}{N_c})$, and $\mathbf{I}_N$ represents the $N \times N$ dimensional identity matrix. A cyclic prefix (CP) is added to the signal $\hat{\mathbf{u}}(a)$ by multiplication with matrix $\mathbf{\Theta}$, which adds the last $N_t N_g$ elements of $\hat{\mathbf{u}}(a)$ on top of $\hat{\mathbf{u}}(a)$. We assume here that the CP is longer than the channel impulse response (CIR), avoiding inter-symbol-interference (ISI). It is assumed that the average total TX power P is divided among the TX antennas such that $\sigma_u^2 = P/N_t$. The signal is then upconverted to radio frequency centered at f_{LO}^{TX} and transmitted through the quasi-static multipath channel $\mathbf{C}$. The average channel or propagation attenuation is assumed to be $\sigma_c^2 = 1$. At the RX the signal is down converted to baseband

with the local oscillator centered at f_{LO}^{RX}, where the a-th received $N_c N_r \times 1$ time domain symbol is given by $\hat{\mathbf{r}}(a) = \text{vec}\left(\mathbf{r}(a \cdot (N_c + N_g)), \ldots, \mathbf{r}((a+1) \cdot (N_c + N_g) - 1)\right)$, where $\mathbf{r}(m)$ denotes the $N_r \times 1$ receive vector at sample instant m. The CP is removed (Rmv CP) by multiplication with $\mathbf{\Theta}^{-1}$, which removes the first $N_r N_g$ elements of $\hat{\mathbf{r}}(a)$. The received signal $\hat{\mathbf{y}}$ is converted to the frequency domain using the DFT, when the CFO is zero, thus $\Delta f = f_{LO}^{TX} - f_{LO}^{RX} = 0$, this yields

$$\begin{aligned}\hat{\mathbf{x}}(a) &= (\mathbf{F} \otimes \mathbf{I}_{N_r})\hat{\mathbf{y}}(a) = (\mathbf{F} \otimes \mathbf{I}_{N_r})\mathbf{\Theta}^{-1}\hat{\mathbf{r}}(a) \\ &= (\mathbf{F} \otimes \mathbf{I}_{N_r})\mathbf{\Theta}^{-1}(\mathbf{C}\mathbf{\Theta}(\mathbf{F}^{-1} \otimes \mathbf{I}_{N_t})\hat{\mathbf{s}}(a) + \hat{\mathbf{v}}(a)) \\ &= \hat{\mathbf{H}}\hat{\mathbf{s}}(a) + \hat{\mathbf{n}}(a) \ , \end{aligned} \tag{2}$$

where $\bar{\mathbf{C}} = \mathbf{\Theta}^{-1}\mathbf{C}\mathbf{\Theta}$ is a *block circulant matrix* signifying the time domain MIMO channel, which can be diagonalized by the IDFT and DFT operation [14] yielding the $N_c N_r \times N_c N_t$ block diagonal matrix $\hat{\mathbf{H}}$. The n-th $N_r \times N_t$ block diagonal element is $\mathbf{H}(n)$, the $N_r \times N_t$ MIMO channel of the n-th subcarrier. $\hat{\mathbf{n}}(a)$ represents the frequency-domain noise, with i.i.d. zero-mean, complex Gaussian elements and $\hat{\mathbf{v}}(a)$ denotes its time-domain equivalent. The variance of the elements of $\mathbf{v}(m)$ is σ_v^2. It is clear from (2) that the carriers are orthogonal.

When frequency offset occurs, thus $\Delta f \neq 0$, the received frequency domain signal is given by

$$\begin{aligned}\hat{\mathbf{x}}(a) &= (\mathbf{F} \otimes \mathbf{I}_{N_r})\mathbf{\Theta}^{-1}(\mathbf{E}\mathbf{C}\mathbf{\Theta}(\mathbf{F}^{-1} \otimes \mathbf{I}_{N_t})\hat{\mathbf{s}}(a) + \hat{\mathbf{v}}(a)) \\ &= (\mathbf{G} \otimes \mathbf{I}_{N_r})\,\hat{\mathbf{H}}\hat{\mathbf{s}}(a) + \hat{\mathbf{n}}(a) \ , \end{aligned} \tag{3}$$

where $\mathbf{E} = \text{diag}(e_0, e_1, \ldots, e_{N_c+N_g-1}) \otimes \mathbf{I}_{N_r}$ denotes the phase rotation due to the CFO, with $e_m = \exp\left(j2\pi\Delta f T_s(a(N_c + N_g) + m)\right)$. Here we assumed that the phase offset at the start of the packet is part of the channel. T_s denotes the sample time. From (3) it is clear that $\mathbf{\Theta}^{-1}\mathbf{E}\mathbf{C}\mathbf{\Theta}$ is no longer block circulant and can thus not be diagonalized by the DFT and IDFT operations. The $N_c \times N_c$ matrix $\mathbf{G}$ in (3) shows the influence of the CFO on the received frequency domain symbols and is given by

$$\mathbf{G} = \begin{pmatrix} g_0 & g_{-1} & \cdots & g_{-(N_c-1)} \\ g_1 & g_0 & \cdots & g_{-(N_c-2)} \\ \vdots & \vdots & \ddots & \vdots \\ g_{N_c-1} & g_{N_c-2} & \cdots & g_0 \end{pmatrix} \ , \tag{4}$$

where

$$\begin{aligned} g_q = \ & \frac{\sin(\pi(\delta - q))}{N_c \sin(\frac{\pi}{N_c}(\delta - q))} \cdot \exp\left(j\frac{\pi(N_c - 1)}{N_c}(\delta - q)\right) \\ & \cdot \exp\left(j\frac{2\pi\delta}{N_c}(a(N_c + N_g) + N_g)\right) \ , \end{aligned} \tag{5}$$

where $\delta = \Delta f N_c / f_s$ is the frequency offset normalized to the subcarrier spacing. We clearly see the following effects of frequency offset: the wanted carriers, multiplied with g_0, are rotated and their amplitude is reduced, and the other elements of $\mathbf{G}$, thus for $q \neq 0$, introduce cross terms which result in ICI.

III. Frequency Synchronization

To reduce these effects of CFO, accurate synchronization is important, preferably before reception of the data. Therefore the datapacket is preceded by a section of predefined data, which is called the preamble. MIMO channel estimates are also drawn from the preamble.

A. Preamble design

The preamble is used for both frequency synchronization and channel estimation. For the proposed frequency synchronization algorithm a repetition of the training symbol is required. For the estimation of the MIMO channel, it is important that the subchannels from the different TX antennas to every RX antenna can be uniquely identified. To achieve that, the preambles on the different TX antennas have to be orthogonal and shift-orthogonal for at least the channel length.

To meet these requirements we propose the use of constant-envelope orthogonal codes with good periodic correlation properties, such as Frank-Zadoff codes [15]. The periodic correlation function Ψ of the code sequence $\mathbf{c} = \{c_1, c_2, ..., c_{N_p}\}$ of length N_p is defined as $\Psi_i = \sum_{k=1}^{N_p} c_{k+i} c_k^*$, where $c_{m+N_p} = c_m$ and * denotes the complex conjugate. For the Frank-Zadoff codes this periodic correlation yields $\sum_{k=1}^{N_p} |c_k|^2$ for $i = 0$ and zero for all other values of i.

The preamble is formed by a repetition of the code, or training symbol, with a different cyclic shift applied to it for the different transmit antennas. A typical value of the cyclic shift would be $\lfloor N_p/N_t \rfloor$. Note that this cyclic shift has to be higher than the CIR length to preserve orthogonality. Altogether, this results in a preamble as depicted in Fig. 2 for a system with two TX antennas.

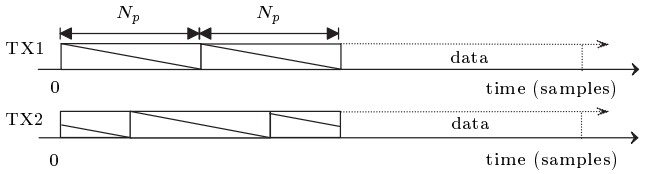

Fig. 2. Concept of preamble for a MIMO configuration with two TX.

B. Synchronization algorithm

To regain the orthogonality between the MIMO OFDM carriers we have to correct for $\mathbf{E}$ in (3) before applying the DFT operation, as shown in Fig. 1. The goals is thus estimating $\mathbf{E}$ and multiplying the received time domain sequence with $\mathbf{E}^{-1}$. The only unknown parameter in $\mathbf{E}$ is the CFO Δf. Moose showed in [6] how Δf can be estimated for a SISO OFDM system using the phase of the complex correlation between two consecutive received versions of a training symbol.

Rather than estimating the CFO on every RX branch separately and then averaging over the different estimates, we propose a way which exploits the receiver diversity for the estimation without using knowledge of the MIMO channel. To that end, we define the complex correlation Λ between two subsequently received frames of N_p samples on the N_r RX antennas as

$$\Lambda(m) = \sum_{k=m}^{m+N_p-1} \mathbf{r}^H(k)\mathbf{r}(k+N_p) \ , \tag{6}$$

where ^{H} denotes the conjugate transpose. The estimated frequency offset Δf_{est} is given by

$$\Delta f_{\text{est}} = \frac{\theta_{\text{est}}}{2\pi T_p} = \frac{f_s \angle\Lambda(\tau_p)}{2\pi N_p} \ , \tag{7}$$

where $\theta_{\text{est}} = \angle\Lambda$ denotes the phase of the complex correlation Λ between two training symbols, f_s denotes the sample frequency and $T_p = N_p/f_s$ the training symbol duration. The best instant to estimate this frequency offset is at τ_p, where $|\Lambda|$ reaches its maximum.

In a multipath environment this estimator achieves a maximum ratio combining (MRC) like performance, since the contribution of the RX branches to Λ is proportional to the received power on the different branches. Clearly the RX branch with the highest instantaneous signal-to-noise ratio (SNR), when assuming a fixed noise floor, contributes most to the estimation of Δf_{est}. This MRC-like performance decreases for lower SNR, since there the contributions are less correlated with the received power due to the influence of receiver noise. This receiver diversity performance is explored by means of simulation results in Section V.

Note that the maximum estimated frequency offset is limited, since the angle θ_{est} that can be estimated without phase ambiguity is limited to $\theta_{\max} = \pm\pi$. This relates to a maximum frequency offset of $|\Delta f_{\max}| = \theta_{\max} f_s/2\pi N_p = f_s/2N_p$. Larger ranges can be achieved by first performing a coarse CFO estimation by preceding the preamble with training symbols with shorter length N_p, as done in [1].

IV. Analytical Results

As a measure of accuracy for the estimator we regard the theoretical value of the variance of the estimate. Moose derived this in [6] for the SISO estimator in an Additive White Gaussian Noise (AWGN) channel. Here we extend this evaluation for the above described MIMO version of the estimation algorithm. The correlation output Λ in an AWGN environment is given by

$$\Lambda(m) = \sum_{k=m}^{m+N_p-1} \{\mathbf{t}(k)+\mathbf{v}(k)\}^H \{\mathbf{t}(k+N_p)+\mathbf{v}(k+N_p)\} \ , \tag{8}$$

where $\mathbf{t}$ and $\mathbf{v}$ are the $N_r \times 1$ received signal and noise vector, respectively, as depicted in Fig. 1. The noise causes an error in the phase estimation of the correlation value Λ. The error in the estimation of the phase is expressed by

$$\theta_{\text{est}} - \theta = \tan^{-1}\left\{\frac{\Im\left(e^{-j\theta}\Lambda\right)}{\Re\left(e^{-j\theta}\Lambda\right)}\right\} \ , \tag{9}$$

where θ denotes the perfect estimation. $\Im$ and $\Re$ denote the imaginary and real part, respectively. Applying (7) and making an approximation for high SNR, we find the following expression for the error in the normalized frequency offset estimation

$$\varepsilon \approx \frac{\sum_{k=m}^{m+N_p-1} N_c \Im\left(\mathbf{t}(k)\mathbf{v}^H(k) + \mathbf{t}^H(k)\mathbf{v}(k+N_p)e^{-j\theta}\right)}{\sum_{k=m}^{m+N_p-1} 2\pi N_p \|\mathbf{t}(k)\|^2} \ , \tag{10}$$

where $\varepsilon = (\Delta f_{\text{est}} - \Delta f)/(\Delta F)$ and $\Delta F = f_s/N_c$ denotes the subcarrier spacing. The mean of ε is zero, consequently the estimator is unbiased. The normalized variance of the estimator, is then found to be

$$\text{var}\,(\varepsilon) = E\left(\varepsilon^2\right) = \frac{N_c^2}{(2\pi)^2 N_r N_p^3 \rho} \ , \tag{11}$$

where $\rho = N_t\sigma_u^2/\sigma_v^2 = P/\sigma_v^2$ denotes the SNR per receive antenna and $E(x)$ denotes the expected value of x. The variance of the estimator equals the (mean square error) MSE, since the estimator is unbiased. It is clear from (11) that the MSE decreases linearly with the number of receive antennas (N_r) and cubically with the training symbol length (N_p).

To check the optimality of the algorithm we derived the Cramér-Rao lower bound for the MIMO frequency offset estimator in an approach similar to [16], as was done for the SISO version in [7]. It turns out to be given by

$$\text{var}\,(\varepsilon) \geq \frac{N_c^2}{(2\pi)^2 N_r N_p^3 \rho} \ . \tag{12}$$

The Cramér-Rao lower bound thus equals the theoretical value of the variance, which means it is the Maximum-Likelihood estimator, as concluded before for the SISO version in [6].

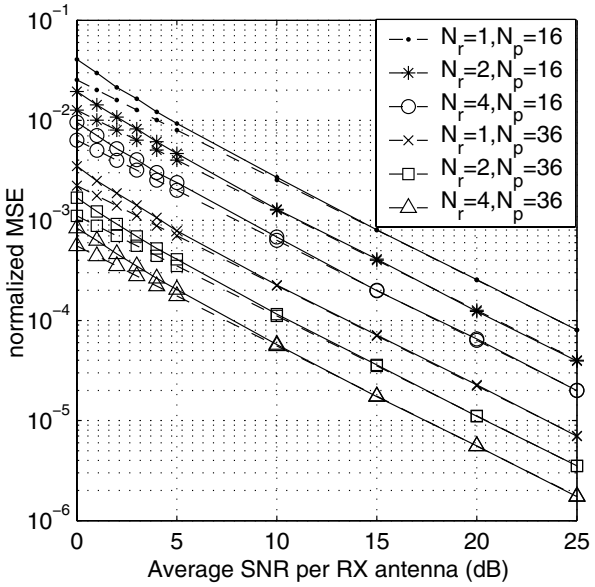

Fig. 3. Theoretical (−−) and simulated (—) MSE of the CFO estimation for different combinations of N_p and N_r as function of the SNR for AWGN channels.

TABLE I
SIMULATION PARAMETERS, BASED ON IEEE 802.11A [1]

System Parameter	Paramater Value
Modulation	BPSK
Coding Rate	1
Bandwidth	20 MHz
Number of subcarriers	64
Number of data subcarriers	48
OFDM Symbol duration	4 μs
Guard Interval	800 ns

Analytical results for the MSE as function of the SNR are depicted in Fig. 3 for different values of N_p and N_r together with the results of the corresponding simulation results with perfect orthogonal AWGN channels. The number of TX antennes was chosen to be equal to N_r and the CFO δ was 0.2 in the simulations, although it is noted the MSE does not depend on N_t and δ (when $|\delta| < N_c/2N_p$) in the AWGN case. Other parameters are set to values given in Table I.

It is clear from Fig. 3 that the theoretical value, which equals the Cramér-Rao lower bound, is a good estimate of the variance for high SNR values, but underestimates the variance compared to simulation results for low SNRs, which is caused by the approximation going to (10). The 6 dB decrease in variance expected from (11), when going from a 1×1 to a 4×4 configuration, is also observable. More gain in variance is achieved when increasing the training symbol length N_p: going from $N_p = 16$ to $N_p = 36$ gains 10.6 dB.

For a given configuration and SNR range an optimal code-length N_p can now be chosen, using (11) and Fig. 3, finding a compromise between accuracy, the maximum offset that can be estimated and the preamble length.

V. SIMULATION RESULTS

To further evaluate the performance of frequency synchronization, simulations are performed with several antenna configurations and delay spreads. The CIRs of all channel elements (i.e. the channel between a certain transmit and receive antenna) are modeled using an exponentially decaying power delay profile (PDP) with independent Rayleigh fading on every tap [14]. The MIMO channel elements are assumed to be independent.

For all simulations a preamble in accordance with Section III-A is applied, with a total length of $2 \cdot N_p = 2 \cdot 64$ samples. On every antenna a CP of 32 samples is added to that. A cyclic shift of $(i-1)64/N_t$ samples is applied to obtain the training sequence for the i-th TX antenna. The preamble is followed by random OFDM data. Other parameters are chosen according to the IEEE 802.11a standard, as shown in Table I. The CFO δ was set to 0.2. For all results 10000 independent realizations were simulated.

Figure 4 shows the normalized MSE of the CFO estimation as function of the average SNR per receive antenna. The theoretical AWGN value from (11) is depicted together with results from Monte-Carlo simulations with both AWGN channels and channels with the exponentially decayed PDP having different values of rms delay spread (tds). The figure depicts these results for the SISO and the 4×4 MIMO configuration.

The simulations with multipath channels show a degradation in performance from the theoretical and the simulated AWGN case. The degradation is highest for the 10 ns case and decreases when the rms delay spread increases. This can be explained by the frequency diversity which is introduced at higher delay spreads. The degradation, however, is much smaller in the 4×4 case than in the SISO case. This can be explained by the fact that even for the low tds case we already have a diversity gain, namely the spatial diversity.

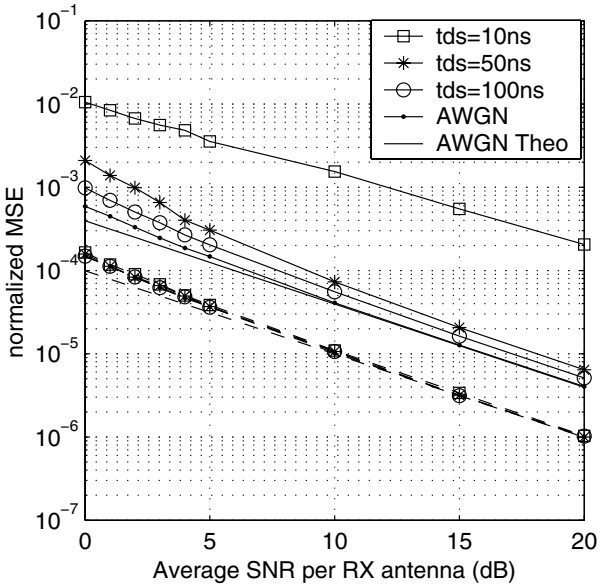

Fig. 4. Variance of the frequency offset estimate for a 1×1 (—) and a 4×4 (−−) system from theory and simulations with AWGN and multipath channels.

To further study the impact of the multiple antennas, Fig. 5 shows the gain in MSE for a MIMO system over the SISO system as function of the rms delay spread for an average SNR of 20 dB. Clearly the highest gain is achieved at low delay spreads. For high rms delay spreads the improvement goes towards the improvement found for AWGN, i.e. $10\log_{10}(N_r)$ dB. The decrease in improvement as function of delay spread is caused by the increasing frequency diversity. When the frequency diversity is high, the addition of TX or RX diversity does not gain significantly compared to the gain in case of AWGN. The results also show that the gain of the MIMO configurations is more than $10\log_{10}(N_r)$ dB higher than the corresponding case with only TX diversity, showing the influence of the mentioned MRC like performance.

The impact of the proposed frequency synchronization approach on the overall system performance is illustrated by means of an example in Fig. 6. It shows the raw bit-error-rate (BER) (without coding) for 1×1, 2×2 and 4×4 systems, respectively, applying VBLAST [17] as MIMO detection algorithm for both perfect synchronization and for the implementation of the above described synchronization.

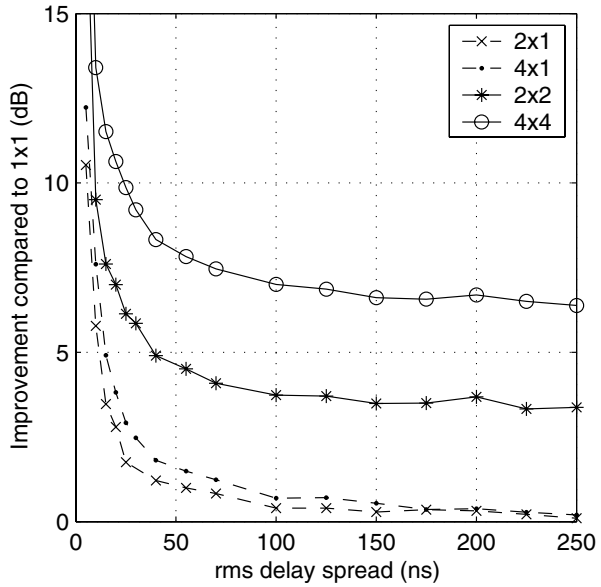

Fig. 5. Improvement in MSE for different configurations compared to 1×1.

The packetlength is 16 μs, i.e. 4 MIMO OFDM symbols, independent of the MIMO configuration. For the simulations, uncorrelated multipath channels with a rms delay spread of 50 ns are applied. To show only the influence of the frequency synchronization, the channel estimation is assumed perfect.

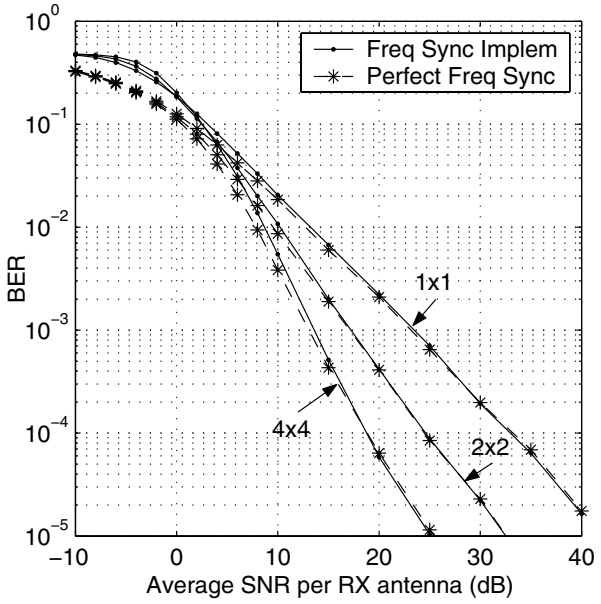

Fig. 6. Performance of VBLAST algorithm applying perfect (−−) and implemented synchronization (—) for a 1×1, 2×2 and 4×4 configuration.

It is clear from the results in Fig. 6 that the implementation of the frequency synchronization causes some degradation in performance at low SNR, which can be explained by the poor estimation of the frequency offset at these SNR values. In the BER range of interest, however, the degradation compared to perfect synchronization is very small.

VI. Conclusions

An efficient burst frequency synchronization for a system combining MIMO with OFDM was proposed and analyzed. A suitable MIMO preamble scheme consisting of orthogonal codes with good periodic correlation properties is defined which is also suitable for MIMO channel estimation. The CFO estimation algorithm is based on exploiting the repetitive nature of the preamble. The theoretical derivation of the accuracy shows that MSE decreases linearly with the number of RX antennes and cubically with the training symbol length in an AWGN environment. In multipath environments a large increase in performance is achieved (compared to the SISO version of the algorithm) by the space diversity that is introduced by MIMO.

The suitability of the proposed synchronization approach was shown through performance simulations of a MIMO OFDM WLAN system, which resulted in only a slightly higher BER than a perfectly synchronized system.

References

[1] IEEE 802.11a standard, ISO/IEC 8802-11:1999/Amd 1:2000(E).

[2] IEEE 802.11g standard, Further Higher-Speed Physical Layer Extension in the 2.4 GHz Band.

[3] G.J. Foschini and M.J. Gans, "On limits of wireless communications in a fading environment when using multiple antennas", *Wireless Personal Communications*, vol. 6, no. 3, pp. 311-335, March 1998.

[4] A. van Zelst, R. van Nee and G.A. Awater, "Space Division Multiplexing (SDM) for OFDM systems", *IEEE Vehicular Technology Conf. 2000-Spring*, pp. 1070-1074, May 2000.

[5] T. Pollet, M. V. Bladel, and M. Moeneclaey, "BER sensitivity of OFDM systems to carrier frequency offset and Wiener phase noise", *IEEE Trans. on Communications*, vol. 43, pp. 191-193, Feb./Mar./Apr. 1995.

[6] P.H. Moose, "A Technique for Orthogonal Frequency Division Multiplexing Frequency Offset Correction", *IEEE Trans. on Communications*, vol. 42, no. 10, pp. 2908-2914, Oct. 1994.

[7] T.M. Schmidl and D.C. Cox, "Robust Frequency and Timing Synchronization for OFDM", *IEEE Trans. on Communications*, vol. 45, no. 12, pp. 1613-1621, Dec. 1997.

[8] G. Santella, "Frequency and symbol synchronization system of OFDM signals: Architecture and simulation results", *IEEE Trans. on Vehicular Technology*, vol. 49, no. 1, pp. 254-275, Jan 2000.

[9] H. Liu and U. Tureli, " A high efficiency carrier estimator for OFDM communications", *IEEE Communication Letters*, vol. 2, no. 4, pp. 104-106, April 1998.

[10] J. van de Beek, M. Sandell and P.O. Borjesson, "ML estimation of time and frequency offset in OFDM systems", *IEEE Trans. on Signal Processing*, vol. 45, no. 7, pp. 1800-1805, July 1997.

[11] A. Czylwik, "Synchronisation for systems with antenna diversity", *IEEE Vehicular Technology Conf. 1999*, vol. 2, pp. 728-732, 1999.

[12] A.N. Mody and G.L. Stüber, "Synchronization for MIMO OFDM Systems", *IEEE Global Communications Conference 2001*, vol. 1, pp. 509-513, Nov. 2001.

[13] U. Tureli, D. Kivanc and H. Liu, "Multicarrier synchronization with diversity", *IEEE VTC Fall Conf. 2001*, vol. 2 pp. 952-956, Oct. 2001.

[14] A. van Zelst and T.C.W. Schenk, "Implementation of a MIMO OFDM based Wireless LAN System", *Accepted for publication in IEEE Trans. on Signal Processing*, 2003, available from htpp://tte.ele.tue.nl/radio/SchenkT.html.

[15] R.L. Frank and S.A. Zadoff, "Phase Shift Pulse Codes With Good Periodic Correlation Properties", *IRE Trans. on Information Theory*, vol. IT-8, pp. 381-382. 1962.

[16] D. Rife and R. Boorstyn, "Single-tone parameter estimation from discrete-time observations", *IEEE Trans. on Information Theory*, IT-20, no. 5, pp. 591-598, Sept. 1974.

[17] P.W. Wolniansky, G.J. Foschini, G.D. Golden and R.A. Valenzuela, "V-BLAST: an architecture for realizing very high data rates over the rich-scattering wireless channel", *Proc. 1998 URSI International Symposium on Signals, Systems, and Electronics*, pp. 295-300, 1998.